Indian J Med Res 146, July 2017, pp 126-137
DOI: 10.4103/ijmr.IJMR_927_15

Quick Response Code:

Bisphenol A-induced ultrastructural changes in the testes of common marmoset

Tushara Vijaykumar†, Dipty Singh†, Geeta R. Vanage, Rohit V. Dhumal & Vikas D. Dighe

National Centre for Preclinical Reproductive & Genetic Toxicology, ICMR-National Institute for Research in Reproductive Health, Mumbai, India

Received June 12, 2015

***Background & objectives*: Bisphenol A (BPA) is an endocrine disruptor that is widely used in the manufacture of polycarbonate plastics, epoxy resins and dental sealants. It is known to have adverse effects on spermatogenesis in rodents. This study was aimed to evaluate the effects of BPA in adult common marmoset owing to its similarities with human spermatogenesis.**

***Methods*: Sixteen marmosets were divided into four groups (n=4 per group) and given oral doses of BPA (2.5, 12.5 and 25 µg/kg BW/day) for 70 days to cover two spermatogenic cycles, and the control group received only vehicle (honey). Testes were processed for histological and transmission electron microscopy studies.**

***Results*: Histology of the testis showed sloughing of germ cells into the lumen, increase in interstitial space and vacuolation of Sertoli cell cytoplasm. Ultrastructural analysis of the testis revealed several degenerative effects on the basement membrane, Sertoli cells, Leydig cells and other developing germ cells in the 12.5 and 25 µg/kg BW/day groups as compared to control.**

***Interpretation & conclusions*: The observed ultrastructural changes caused by BPA in testicular morphology might be indicative of a perturbed sperm production. Considering the genetic and spermatogenic similarities of common marmoset (*Callithrix jacchus*) and humans, the study findings are of significance. Further studies are, however, needed to elucidate the mechanism of action.**

Key words BPA - electron microscopy - endocrine disruptor - marmoset - spermatogenesis - toxicity

Increasing incidences of impaired reproductive functions in humans and animals, observed over the past few decades, have raised concerns about certain chemicals known as endocrine disruptors (EDs)[1]. Recent evidence shows that even low-dose exposure to EDs causes adverse effects to human health[2]. One of these EDs is bisphenol A (BPA), a monomer widely used in the synthesis of various polycarbonate plastics. A large amount of evidence links exposure of BPA to endocrine disruption in laboratory animals and various reproductive health disorders in humans[1]. An earlier study using rats has shown adverse effects of BPA exposure even at low-dose range[3]. A significant decrease in testis and epididymal weight was reported in adult male Wistar rats exposed orally for 45 days to 0.2, 2 and 20 µg/kg body weight (BW)/day, while

†These authors contributed equally to this work

an increase in ventral prostate weight occurred at all doses[4]. Oral administration of BPA (2-200 ng/kg BW) for six days showed decreased sperm count and affected testicular weight and structure in adult male rats[5]. A previous study from our laboratory demonstrated that perinatal exposure to BPA led to alterations in the testicular expression profile of steroid receptor coregulators in the testis[6]. Even neonatal exposure of male rats to BPA caused alterations in the expression of Sertoli cell junctional protein, leading to impairment in spermatogenesis[7].

Severe deformations of the acrosome and spermatid nucleus along with abnormal ectoplasmic specialization in BPA-treated rat testis were observed[8,9]. An ultrastructural analysis demonstrated the presence of vacuoles in mitochondria of spermatids, Sertoli, Leydig and peritubular myoid cells on postnatal day 21 of ICR mice treated with 100 nmol/l of BPA[10]. It has been argued that results derived from these studies cannot be extended to humans due to dissimilarities between rodent and human endocrine systems[11]. Considering this, an animal model more proximal to humans in terms of its reproductive parameters is required to assess the effects of BPA on the reproductive functions. Common marmoset (*Callithrix jacchus*) is a New World monkey, belonging to *Callitrichidae* subfamily. Marmosets have been used in developmental or reproductive toxicity studies owing to its spermatogenic organizational similarities to humans and are proposed as a suitable model for investigating spermatogenesis[10,12]. The present study was, therefore, undertaken to elucidate the effects of BPA on the testis of common marmosets.

Material & Methods

The experiments were performed at the National Institute for Research in Reproductive Health (NIRRH), Mumbai, India. Sixteen adult male marmosets bred in our colony were selected for the study. Animals were housed individually in stainless steel cages and maintained under controlled temperature (23°C±1°C) and humidity (55%±5%) and in a 14 h light/10 h dark cycle. The monkeys were fed daily on a diet consisting of an apple or an orange or a sweet lime, bread, whole milk powder and bananas. Dry dates, egg, vitamin D_3 (2500 IU/animal), vitamin B_{12} (0.5 ml/animal), multivitamin drops (0.25 ml/animal) and calcium solution (0.2 ml) were also provided. Water was provided *ad libitum*. The study was approved by the Institutional Animal Ethics Committee (IAEC/NIRRH/07/10) with a nominee from Committee for the Purpose of Control and Supervision on Animals (CPCSEA).

BPA was procured from Sigma Chemical Co., USA. Sodium cacodylate buffer, araldite, dodecenyl succinic anhydride, 2,4,6-tri(dimethyl aminomethyl) phenol, uranyl acetate and osmium tetraoxide (OsO_4) were procured from Ted Pella Inc., USA.

Dose selection: The BPA doses were selected based on previous toxicokinetic study in marmoset (unpublished data). Primates have been considered as good model owing to its similarity to humans in hepatic blood flow rate. BPA at 10 µg/kg BW was administered to marmosets (n=2) orally. Blood (0.2-3 ml) was collected from the femoral vein at 0.15, 0.30, 1, 2, 4, 6 and 24 h time points after BPA administration. The maximal plasma BPA concentration (C_{max}) achieved was 204 ng/ml in one hour (T_{max}) (Fig.1). The safe human exposure dose reported by the National Toxicology Programme is 2.4 µg/kg BW/day[13]. Based on our toxicokinetic study (unpublished data), we selected doses 2.5, 12.5 and 25 µg/kg BW/day to study the effects on spermatogenesis in adult marmoset.

Experimental design: BPA was dissolved in a small volume of ethanol (99% pure) and was then suspended in honey to obtain the desired concentrations of 2.5, 12.5 and 25 µg/kg BW/day. Sixteen adult male marmosets weighing 300-450 g on an average were divided into four groups (four animals/group), Group I: vehicle control (honey), Group II: BPA 2.5 µg/kg/day, Group III: BPA 12.5 µg/kg/day and Group IV: BPA 25 µg/kg/day. All marmosets were orally fed with these doses for 70 days to cover two complete spermatogenic cycles.

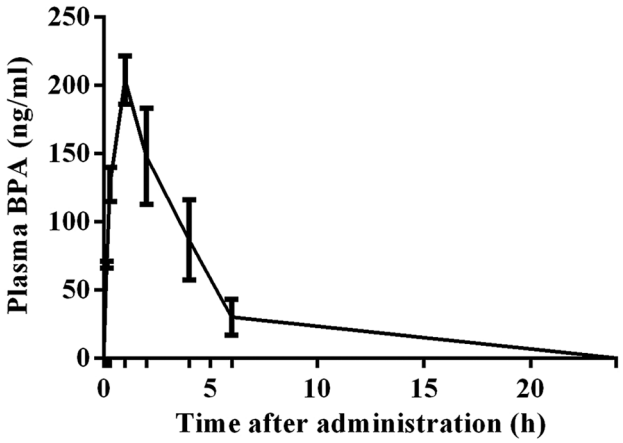

Fig. 1. Toxicokinetic study of bisphenol A in plasma from adult male marmoset during the 24 h after oral administration at10 mg/kg body weight (BW) dose. The C_{max} was 204 ng/ml at one hour (T_{max}).

Haematology, serum and hormonal parameters: At the end of the treatment, 1 ml blood was drawn from the femoral vein for analysis of various haematology and serum biochemical parameters. The testosterone and oestrogen levels were analyzed on AIA 360 Automated Immunoassay Analyzer (Tosoh Bioscience, USA) using ST-AIA PACK competitive enzyme immunoassay(Tosoh Bioscience, USA). An assay was performed using the manufacturer's instructions; briefly, serum samples from control and treatments group were incubated with testosterone/E2-specific monoclonal antibody immobilized on a magnetic solid phase. The magnetic beads were washed to remove unbound enzyme-labelled testosterone/E2 and then incubated with a fluorogenic substrate, 4-methyl-umbelliferyl phosphate. The amount of enzyme-labelled testosterone/E2 that binds to the beads was inversely proportional to the testosterone/E2 concentration in the test sample. A standard curve was constructed, and sample concentrations were calculated using respective curves.

Sample collection and processing: Animals from treated and control groups were sacrificed by an excess dose of anaesthesia (thiopental sodium) after 70 days. All vital organs namely- heart, liver, kidney, lung, brain and spleen, were collected and weighed. The testes were sectioned through transverse axis into two halves. Further, one-half of the testis was processed for light microscopy and another half for electron microscopy analysis.

Light microscopy: Testes were fixed in 10 per cent neutral buffered formalin for 48 h and processed in an automatic tissue processor (Leica ASP200, Germany). Paraffin sections (5 µm) were stained with haematoxylin and eosin and examined under light microscopy (Leica AS LMD, Germany). Quantification of germ cell and Sertoli cell (100 tubules per testis) was performed by calculating the percentage of stage frequencies[14].

Transmission electron microscopy: Tissues were sliced into 1-2 mm^3 pieces and fixed in modified Karnovsky's fixative (4% glutaraldehyde + 4% paraformaldehyde + 0.2% picric acid + 0.02% calcium chloride + 0.2 M cacodylate buffer) for four hours at 4°C. Tissue specimens were post-fixed in one per cent OsO_4 in cacodylate buffer (pH 7.2) for two hours at 4°C. Dehydration of the fixed tissues was performed using ascending grades of acetone. Tissues were transferred to epoxy resin (araldite) via toluene[8]. After impregnation with the pure resin, tissue specimens were embedded in the same resin mixture. Ultrathin sections of silver shades (60-70 nm) were cut using an ultramicrotome (Leica Ultracut R, Leica Microsystems, Wetzlar, Germany) and stained with uranyl acetate and lead citrate. Stained sections were finally observed under transmission electron microscope (TECNAI, 12 BT, FEI, USA) operating at 120 KV.

Statistical analysis: For all the toxicological evaluations, the results of the treatment groups were compared with those of the control group using Student's t test.

Results

The animals did not exhibit any treatment-related abnormal clinical signs and symptoms. There was no mortality during the study. Average body weight (in grams) of the animals was 415±28.68, 403±29.09, 405.5±23.17 and 410±51.82 for groups I, II, III and IV, respectively.

Haematology and serum biochemical parameters: There was no significant difference in various haematological parameters in the treatment group as compared to control (Table I). Further, no significant difference in various clinical chemistry parameters was observed, except the lipid profile of the animals treated with 25 µg/kg BW/day of BPA. A significant increase in low-density lipoprotein (LDL) and cholesterol levels was observed without the change in high-density lipoprotein levels in the high-dose (25 µg/kg BW) group (Table II).

Blood hormone levels: A significant ($P<0.05$) decrease in testosterone level was observed in 12.5 and 25 µg/kg BW/day groups as compared to control (Fig. 2A). No significant change was observed in the oestrogen levels of the treated group (Fig. 2B).

Light and electron microscopy analysis: The light microscopy analysis of the testis of the control marmosets exhibited typical arrangement and population of germ cells and Sertoli cells. It showed typical morphology with different stages of spermatogenic cells (Fig. 3A and B). In 2.5 µg/kg BW/day group, no changes were observed and were comparable to the control group (Fig. 3C and D), whereas 12.5 µg/kg BW/day BPA-treated group showed sloughing of germ cells into the lumen and increase in interstitial space (Fig. 4A and B). Quantification data showed a decrease in germ cells number at round spermatid (RS) and elongated

Table I. Mean haematological parameters of control and bisphenol A-treated marmosets

Parameters	Group I (control)	Group II (2.5 µg/kg BW)	Group III (12.5 µg/kg BW)	Group IV (25 µg/kg BW)
WBC ($\times10^3$/µl)	12.68±5.84	14.90±6.66	9.14±1.01	6.21±1.10
RBC ($\times10^6$/µl)	7.99±0.27	8.32±0.57	8.24±0.88	7.46±0.67
HGB (g/dl)	15.05±0.42	15.28±1.05	15.28±1.05	15.35±1.35
HCT (%)	54.00±1.61	55.45±3.95	55.18±5.52	53.88±4.38
MCV (fl)	67.75±3.10	66.75±2.22	67.25±2.75	72.50±1.73
MCH (pg)	18.85±0.87	18.40±1.11	18.65±0.69	20.68±1.98
MCHC (g/dl)	27.850±0.17	27.575±0.89	27.800±0.14	28.525±2.03
PLT (10^3/µl)	489.25±61.14	458.75±75.69	448.25±92.99	436.50±57.51
Neutrophils (%)	36.50±28.99	25.50±15.50	24.75±7.54	44.67±8.39
Lymphocytes (%)	61.50±28.99	72.75±15.33	73.75±6.55	54.00±8.72
Eosinophil (%)	0.50±0.71	0.00±0.00	0.50±0.58	0.00±0.00
Monocytes (%)	1.50±0.71	1.75±0.96	1.00±0.82	0.50±0.58

Values are mean±SD (n=4); SD, standard deviation; BW, body weight; HGB, haemoglobin; RBC, red blood cell; WBC, white blood cell; HCT, haematocrit; MCV, mean corpuscular volume; MCHC, mean corpuscular haemoglobin concentration; PLT, platelet

Table II. Mean clinical chemistry parameters of control and bisphenol A-treated marmosets

Parameters	Group I (control)	Group II (2.5 µg/kg BW)	Group III (12.5 µg/kg BW)	Group IV (25 µg/kg BW)
Albumin (g/dl)	4.90±0.14	4.80±0.25	5.05±0.44	5.23±2.15
Globulin (g/dl)	3.55±0.60	3.38±0.64	4.68±3.18	4.15±0.19
Albumin/globulin ratio	1.43±0.34	1.48±0.26	2.13±1.39	1.78±1.48
Glucose (mg/dl)	141.95±17.73	210.35±84.49	228.30±93.44	263.88±163.42
Cholesterol (mg/dl)	169.50±32.92	190.25±31.69	170.50±11.73	221.75±45.77
HDL (mg/dl)	85.50±18.36	84.00±6.22	80.75±10.05	85.25±30.74
LDL (mg/dl)	81.43±28.97	125.65±37.15	107.83±12.56	169.85±7.83*
Triglycerides (mg/dl)	92±11.97	117.75±76.43	107.5±26.34	101.5±14.55
SGPT (U/l)	19.70±23.58	5.63±2.83	5.48±4.50	4.45±1.78
SGOT (U/l)	257.00±115.02	162.55±50.97	178.10±42.06	165.30±53.0
Creatinine (mg/dl)	0.50±0.08	0.53±0.10	0.60±0.14	0.70±0.34
Urea (mg/dl)	40.60±11.17	40.73±9.20	44.10±8.33	41.90±8.44
Alkaline phosphatase (U/l)	455.55±170.62	533.30±234.30	445.85±192.37	707.85±166.08
Direct bilirubin (mg/dl)	0.30±0.12	0.20±0.08	0.20±0.00	0.33±0.10
Total bilirubin (mg/dl)	0.60±0.25	0.40±0.14	0.65±0.24	0.58±0.21
Total protein (g/dl)	8.45±0.51	8.15±0.66	8.23±0.33	9.40±2.22
Calcium (mg/dl)	11.83±1.16	11.55±0.56	11.85±0.68	13.18±3.49
Phosphorus (mg/dl)	5.30±1.78	5.45±1.46	7.03±2.38	5.55±3.30
Sodium (mmol/l)	157.38±3.38	159.28±3.39	156.83±4.45	151.40±5.53
Potassium (mmol/l)	3.33±0.39	4.23±0.92	4.02±0.19	4.05±1.01

Values are mean±SD (n=4); *P<0.05 compared to control; LDL, low-density lipoprotein; HDL, high-density lipoprotein; SD, standard deviation; BW, body weight; SGOT, serum glutamic-oxaloacetic transaminase; SGPT, serum glutamic-pyruvic transaminase

spermatid (ES) level; however, there was no change in Sertoli cell number observed in this group (Table III). In the case of 25 µg/kg BW/day group, a marked decrease was observed in primary spermatocyte, RS and ES cell numbers, whereas Sertoli cell number did not change. However, intercellular spaces and

Table III. Quantification of germ cell and Sertoli cell numbers

Number of cells (100 tubules/testis×10^6)	Cell type					
	A	B	PS	RS	ES	SC
Control	4±0.6	6.9±1.5	39±3.5	98±7	109±11.5	11±2
12.5 µg/kg BW/day	3.2±0.8	6.4±0.8	32±4	81±9	89±10	12±1
25 µg/kg BW/day	2.7±0.5	5±0.5	23±5*	72±5*	79±8*	9±0.5

Values are mean±SD (n=4); *P<0.05 compared to control; A, A spermatogonia; B, B spermatogonia; PS, primary spermatocyte; RS, round spermatid; ES, elongated spermatid; SC, Sertoli cell; BW, body weight; SD, standard deviation

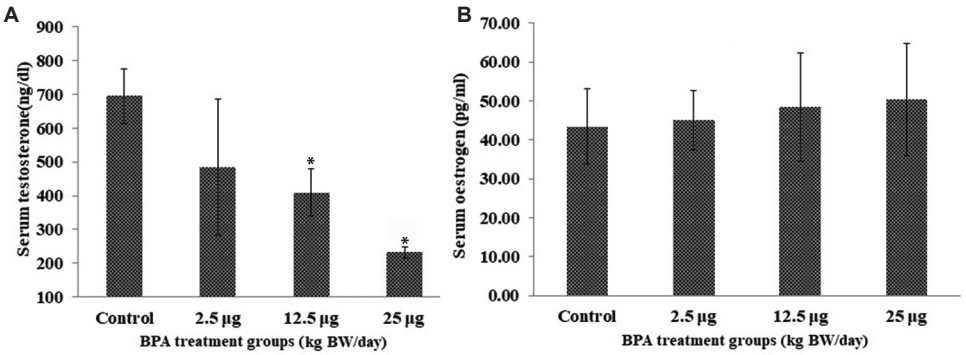

Fig. 2. (**A**) Serum testosterone and (**B**) oestrogen levels. Bars correspond to estimated mean hormone values±standard deviation, N=4, *P<0.05 compared to control.

vacuoles were observed in the cytoplasm of the Sertoli cells in some of the seminiferous tubules (Fig. 4C and D), while the rest of the tubules seemed normal.

Electron microscopic observations revealed alterations in the testicular cells. On analysis, the low-dose (2.5 µg/kg BW/day) group did not show any ultrastructural changes deviant from the control group (data not shown).

Lamina propria: Ultrastructural observation of the control marmoset showed normal lamina propria composed of collagen fibres, peritubular myoid cells and basement membrane. The lamina propria was surrounded by layers of peritubular cells embedded in a framework of collagen (Fig. 5A). As compared to control group, perturbed lamina propria was observed in some of the tissue sections in middle- and high-dose groups. In middle-dose (12.5 µg/kg BW) group, irregular tubular basement membranes with finger-like projections were seen (Fig. 5B and C). High-dose (25 µg/kg BW) group had some vacuolated and degenerated lamina propria (Fig. 5D and E). The lamina propria was more thickened (~6 µm) with fibrous connective tissue than in control groups (~2 µm) (Fig. 5E and F). Collagen fibres were also found to be increased in high-dose group (Fig. 5E).

Sertoli cells: Sertoli cells of the control group were normal with regular nuclear membrane and no evident morphological abnormalities. The Sertoli cells had a deeply indented nucleus, homogeneous nucleoplasm and prominent nucleolus (Fig. 6A). The cytoplasm of the Sertoli cells was extended from the basal lamina to the lumen of the seminiferous tubules having close contact with adjacent germinal elements (Fig. 6B). The cytoplasm contained rosettes of glycogen granules, free ribosome, oval mitochondria, lipid droplets and lysosomes. The Sertoli-to-Sertoli and Sertoli-to-germ cell junctions were intact in case of the control group. By contrast, the BPA-treated 12.5 and 25 µg dose groups showed degenerative changes in Sertoli cell nucleus and the cytoplasm. In 12.5 µg/kg BW/day group, Sertoli cell nucleus was found shrunken with a lot of electron dense secretory products (Fig. 6C). Cytoplasm was vacuolated with degenerating germ cells (Fig. 6D). In 25 µg/kg BW/day group, clear signs of pyknosis were seen in the nucleus such as broken nuclear membrane with fragmented chromatin (Fig. 7A). Sertoli-to-Sertoli and Sertoli-to-germ cell junctions were also severely damaged containing degenerated germ cells in high-dose group (Fig. 7B).

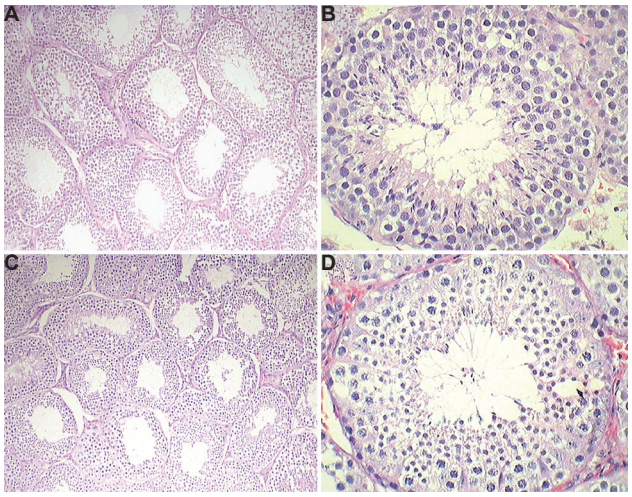

Fig. 3. Representative images of Haematoxylin and Eosin (H & E) stained testis. (**A** and **B**) Control group; (**C** and **D**) 2.5 µg/kg BW group was comparable to the control. (**A** and **C**: ×10 and **B** and **D**: ×40).

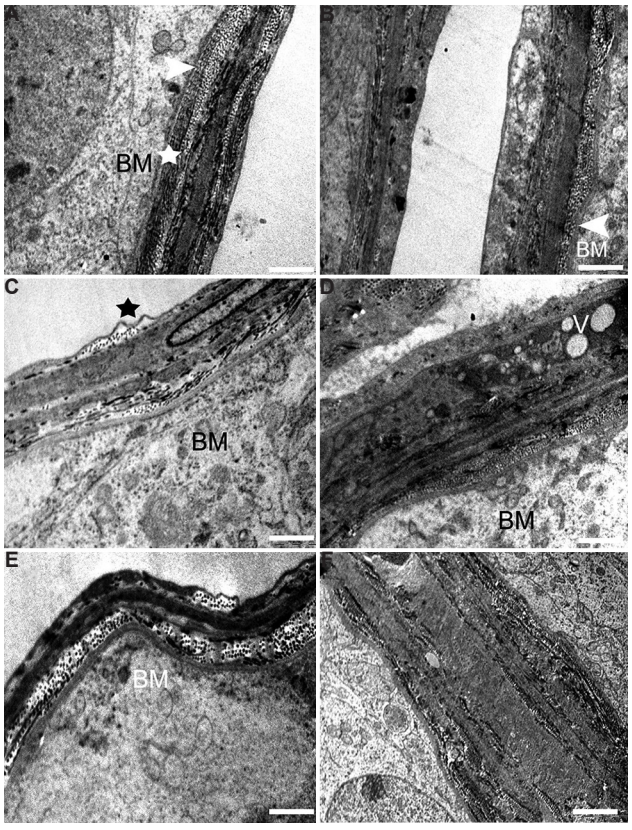

Fig. 5. Electron micrograph of the lamina propria. (**A**) Control testis showing normal lamina propria having collagen fibres (arrowhead), peritubular myoid cells (star) and basement membrane (BM). (**B** and **C**) The testis of 12.5 µg/kg BW group showing signs of damage and fingerlike projections (arrowhead, star) of basement membrane. (**D**) Basal lamina of high-dose group showing vacuolation (V) and thickening of basement membrane, (**E**) increase in collagen fibres and membrane damage, (**F**) highly thickened and vacuolated basal lamina. Scale bar for (**A, B** and **D**) 0.2 µm, (**C**) 1 µm and (**E** and **F**) 2 µm.

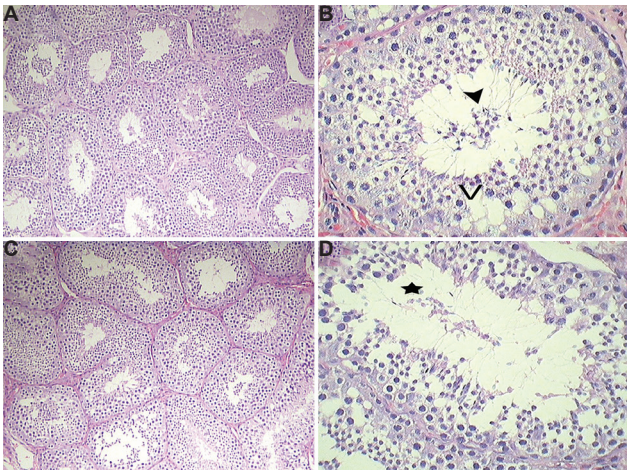

Fig. 4. Representative images of Haematoxylin and Eosin (H & E) stained testis. (**A** and **B**) 12.5 µg/kg BW dose showed sloughing of cells into the lumen (arrowhead) and presence of vacuoles (V) in Sertoli cytoplasm; (**C** and **D**) 25 µg/kg BW group showed disintegration of cellular morphology (star) with reduced mature spermatids. (**A** and **C**: ×10 and **B** and **D**: ×40).

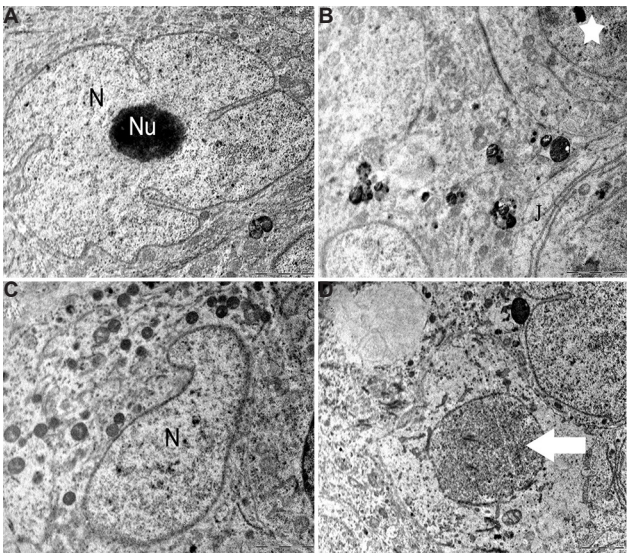

Fig. 6. Testicular ultrastructure of the Sertoli cell. (**A** and **B**) Control animals showing the nucleus (N) and nucleolus (Nu), tight junctions (J) and other intact cellular organelles (star). (**C**) The animals in 12.5 µg/kg BW/day experimental group showing shrunken Sertoli cell nucleus (N) with secretory products. (**D**) Ultrastructure of vacuolated and degenerating germ cells (arrow). Scale bar for all is 2 µm except for (A) is 0.2 µm.

In this group, degenerative changes in the form of necrosis and severe vacuolization were also observed (Fig. 7C and D).

Leydig cells: The electron micrograph of the Leydig cell from the control group had normal cellular organelles and nucleus containing prominent rim of heterochromatin attached to the nuclear membrane

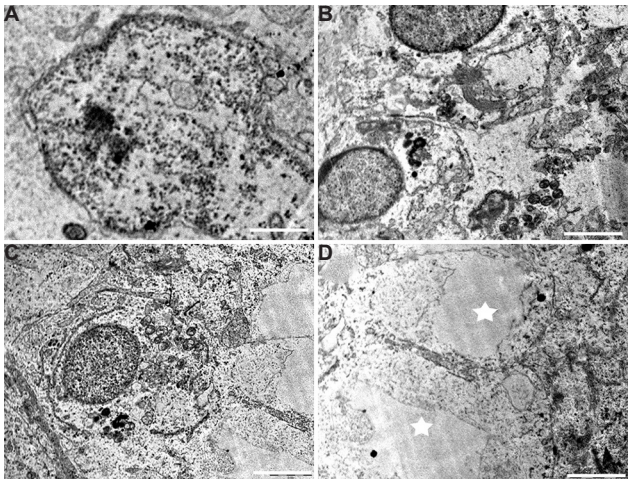

Fig. 7. Testicular ultrastructure of the Sertoli cell in 25 µg/kg BW/day dose group. (**A**) Sertoli cell nucleus showing signs of pyknosis. (**B** and **C**) Testis ultrastructure showing damaged cellular junctions and germ cells. (**D**) Highly vacuolated (star) Sertoli cell cytoplasm in high-dose group. Scale bar for all is 2 µm.

(Fig. 8A) as well as few lipid droplets. Testis ultrastructure of the 12.5 as well as the 25 µg/kg BW/day groups showed greater amounts of lipid droplets distributed all over the cytoplasm. In comparison to the control, Leydig cells of the middle- and the high-dose group had swollen mitochondria and highly granular cytoplasm (Fig. 8B-E).

Spermatogonial cells: Spermatogonial cells of the control marmoset testis were found regularly arranged and with nuclei lying parallel to the tubular membrane. They had a spherical or ovoid nucleus with fine granular nucleoplasm, few mitochondria and plenty of free ribosomes in the cytoplasm (Fig. 9A). The majority of the spermatogonial cells had no signs of abnormality in the control group. However, BPA-treated mid-dose (12.5 µg/kg BW/day) group demonstrated cellular alterations in some spermatogonial cells (Fig. 9B). The cytoplasm of these spermatogonial cells along with surrounding Sertoli cell was relatively damaged having swollen mitochondria, cell debris and vacuoles (Fig. 9B). It was found that a few spermatogonial cells were separated from the basal lamina and neighbouring cells by remarkable spaces (Fig. 9C). However, in the high-dose (25 µg/kg BW/day) group, some spermatogonia showed apoptotic characters, with the observation of shrunken cell (Fig. 9D), condensation and margination of chromatin, leading to the formation of a ring at the inner side of the nuclear envelope. In this group, a few spermatogonia showed nuclear changes as well as apoptosis (Figs. 9E and F).

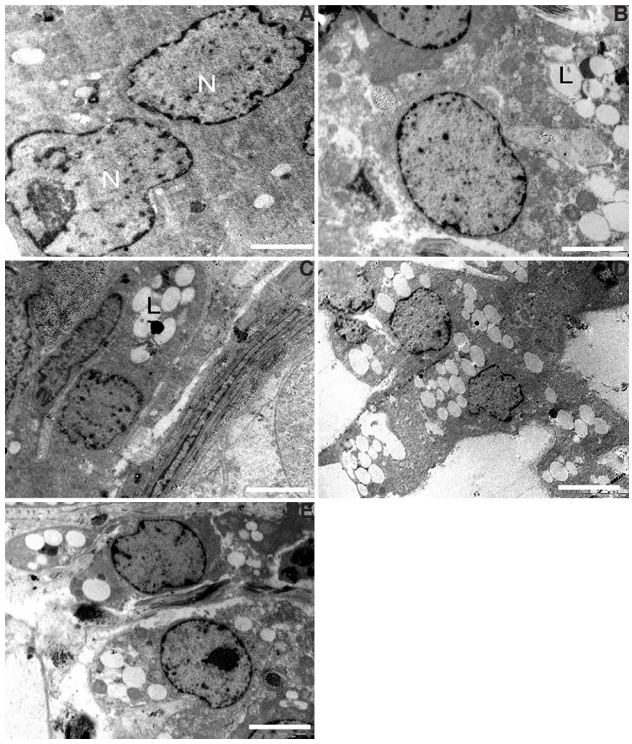

Fig. 8. Electron micrograph of the Leydig cell. (**A**) Control group showing nucleus (N) and cytoplasm. Leydig cell showing high lipid droplets (L) and granular cytoplasm in (**B** and **C**) 12.5 µg/kg BW/day as well as in (**D** and **E**) 25 µg/kg BW/day dose groups. Scale bar for all is 0.2 µm except for C is 2 µm.

Spermatocytes: A number of spermatocytes were noticed in the luminal part of seminiferous tubules in the control testis. These were found separated from the basal lamina by fine processes of Sertoli cell cytoplasm. The spermatocytes displayed round configurations with prominent spherical nuclei (Fig. 10A). The nuclei had granular nucleoplasm and well-defined nuclear envelope. These appeared to have granular cytoplasm, round mitochondria and loose networks of rough endoplasmic reticulum. In contrast to control group, some spermatocytes showed altered nuclear structure containing more than two nucleoli and broken nuclear membrane (Fig. 10B and C). More pronounced signs of spermatocyte apoptosis were seen in higher dose (25 µg/kg BW/day) of BPA-treated group. A part of the nuclear envelope was found missing in a few spermatocyte nucleus (Fig. 10D) accompanied by chromatin condensation (Fig. 10E) and chromatin clumping (Fig. 10F). Some apoptotic spermatocytes were identified with a vacuolated nucleus and degenerated cytoplasmic residues (Fig. 10F).

Round spermatid (RS): RS from the control group was normal, with much smaller nucleus than spermatocyte.

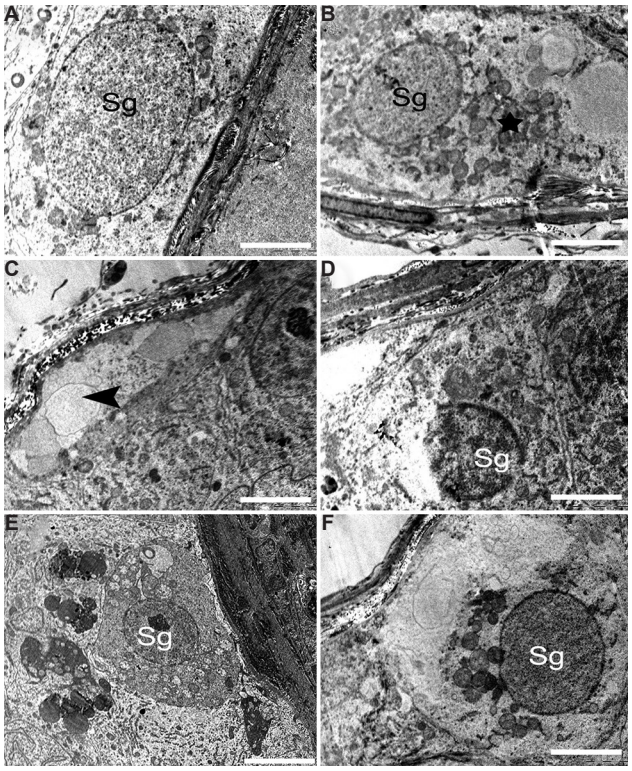

Fig. 9. Electron micrograph of the spermatogonia. (**A**) Control group showing normal spermatogonia (Sg). (**B** and **C**) The animals in 12.5 µg/kg BW/day dose group showed damaged germ cell having swollen mitochondria (star). Spermatogonial cells separated from basal lamina and having large vacuole (arrowhead). (**D-F**) The 25 µg/kg BW/day group showing degenerated spermatogonial cells and apoptotic spermatogonial cells (Sg). (**F**) Spermatogonial cell nucleus with condensed, marginated chromatin (Sg) and having degenerating cytoplasm. Scale bar for all is 2 µm except for B and E is 5 µm.

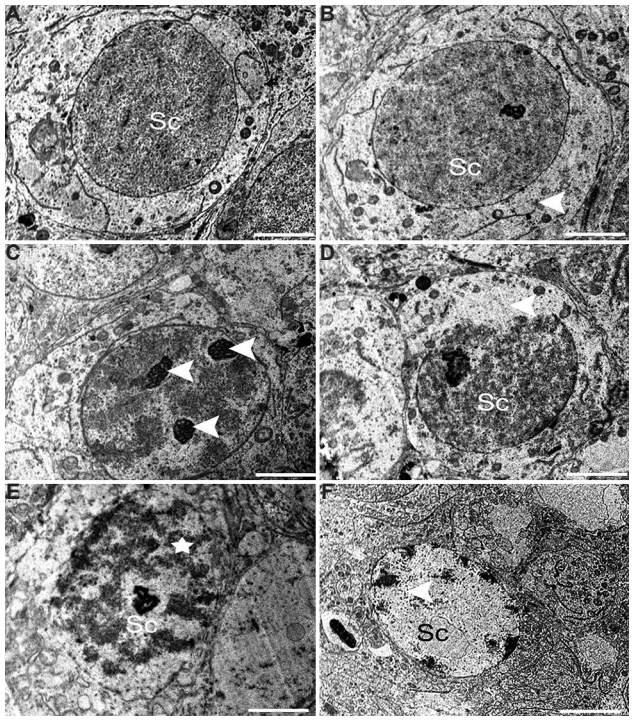

Fig. 10. Electron micrograph of (**A**) the spermatocyte (Sc) from control group with prominent well-defined nucleus and intact granular cytoplasm. (**B** and **C**) Spermatocyte showing degenerative signs having broken nuclear envelope and lipid droplets (arrowheads) and multi nucleoli (arrowhead) in middle dose group. High-dose group showed (**D**) Spermatocyte (Sc) with partly missing nuclear membrane (arrowhead), (**E** and **F**) apoptotic (star), spermatocyte (Sc), (**F**) Spermatocyte (Sc) showing chromatin clumping and nuclear vacuolation (arrowhead). Scale bar for all is 0.2 µm except for F is 2 µm.

Nucleus presented clear nuclear membrane with no evident morphological abnormalities in the mitochondria and other organelles. Spermatids were well surrounded by Sertoli cell cytoplasm having distinct intact cellular junctions (Fig. 11A). The mid-dose (12.5 µg/kg BW/day) BPA-treated testis showed RS with some ultrastructural abnormalities such as margination of chromatin and cytoplasmic vacuoles (Fig. 11B). Cytoplasm surrounding the RS appeared degenerative with enlarged intracellular spaces and electron dense bodies (Fig. 11C). Similar to other germ cells, RS also got affected at the higher dose of BPA treatment. Spermatid and Sertoli cell tight junction appeared disrupted. There were very few cellular organelles found intact in the cytoplasm (Fig. 11D). The high-dose (25 µg/kg BW/day) treatment group had some degenerated spermatids showing shrunken nucleus and cytoplasmic debris (Fig. 11E). At this dose, late stages of apoptosis were seen where the nuclear envelope was missing, accompanied by large cytoplasmic vacuoles (Fig. 11F).

Elongating spermatid: Normal spermiogenesis was marked with healthy elongating spermatids characterized by the presence of a proacrosomal vesicle situated on the pole of the nucleus in control marmoset testis (Fig. 12A). Other developmental steps of spermiogenesis were also observed, which involved flattening of the proacrosomal vesicle against one pole of the spermatid nucleus and synthesis of acrosomal contents. The cytoplasmic organelles of the spermatids had no evident morphological abnormalities in the control group. On the contrary, BPA-treated middle-dose (12.5 µg/kg BW/day) testis presented some degenerated spermatids and Sertoli cell components along with healthy elongating spermatids (Fig. 12B). A few elongating spermatid showed unusual morphology, such as abnormal acrosomal vesicle fused with shrunken Golgi complex (Fig. 12C). Abnormalities in

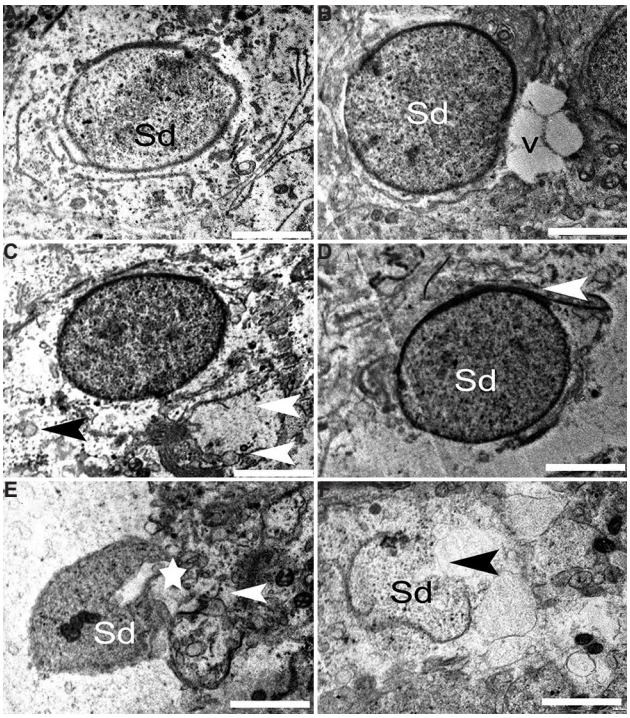

Fig. 11. Electron micrograph of the round spermatid. (**A**) Round spermatid (Sd) from control group having intact ultrastructure. (**B** and **C**) Round spermatid with marginated chromatin, vacuoles (V), necrotic cytoplasm (black arrowhead) and degenerative cellular organelle (white arrowhead) in 12.5 µg/kg BW/day group. (**D-F**) Damaged tight junctions (arrowheads) of round spermatid in 25 µg/kg BW/day dose animals. (**E**) Degenerated spermatid showing shrunken nucleus (star) and cytoplasmic debris (arrowhead). (**F**) At high dose, apoptotic round spermatid was observed. Scale bar for all is 1 µm except for E is 2 µm.

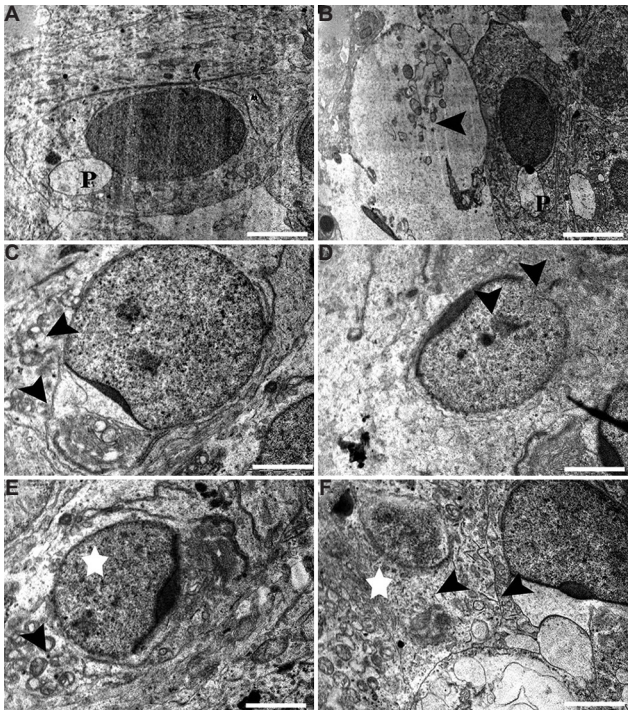

Fig. 12. Electron micrograph of (**A**) Healthy elongating spermatids having developing proacrosomal vesicle (P). (**B** & **C**) Degenerated spermatids and Sertoli cell components (arrowhead) in middle dose group, (**C**) abnormal acrosomal vesicle fused with shrunken Golgi complex (arrowhead). (**D-F**) Condensed granules of chromatin with damaged nuclear envelope (arrowheads) in high-dose group, (**E**) deformations in mitochondria (arrowhead) and cytoplasm (star) and (**F**) deformed acrosomal vesicle in elongating spermatid (arrowhead) and degenerative cytoplasm (star). Scale bar for A, B & F is 2 µm and for C-E is 0.2 µm.

acrosomal vesicles and abnormal nuclear morphology such as condensed granules of chromatin with damaged nuclear envelope were observed in the 25 µg/kg BW/day dose group (Fig. 12D). At this higher dose, a variety of ultrastructural deformations in the cytoplasm of elongating spermatid were marked. The broken cellular components and collapsed mitochondria could easily be observed as a sign of degeneration (Figs. 12E and F). Deformity in acrosomal vesicle was noticed in few spermatids, where large vacuolar structure appeared fused with it (Fig. 12F).

Elongated spermatid (ES): Ultrastructure of the control testis showed many ESs with intact morphology. These had normal ESs with the typical shape of the head, intact cell membranes, acrosomes and homogenous condensed nuclei (Fig. 13A), whereas some spermatids of the BPA-treated group showed ultrastructural deformities. A mid dose (12.5 µg/kg BW/day) of BPA appeared to have adverse effects on developing spermatid population. Among the prime abnormalities noted were acrosomal changes (Fig. 13B) and perturbed integrity of the membrane (Fig. 13C). Further, spermatozoa with abnormal morphology having head defects were observed in the lumen of high-dose (25 µg/kg BW/day) treatment groups. A number of apoptotic spermatids were found in this group that had vacuolated and collapsed membrane around the nucleus (Fig. 13D). Electron micrographs of the testis from the high-dose group showed that deformed elongating spermatids were phagocytized by Sertoli cell, which resulted in engulfed spermatids in the cytoplasm of Sertoli cells (Fig. 13E). An experimental group at the high dose also showed some severely damaged spermatid with head defects and degenerated cytoplasm of surrounding Sertoli cells (Fig. 13F).

Discussion

Widespread use of oestrogenic pollutant BPA in our daily lives led its entry in the food chain[15]. The amount of BPA to which humans are exposed raises

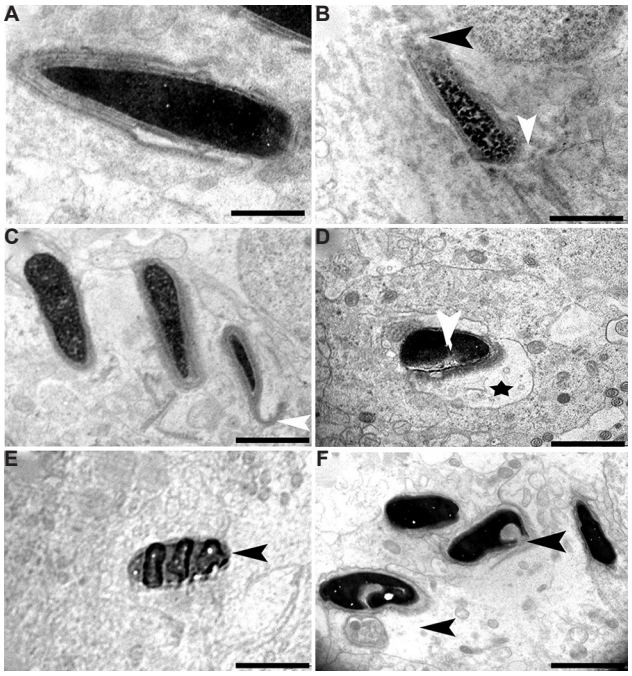

Fig. 13. Electron micrograph of elongated spermatids. (**A**) Transmission electron microscopic image showing control group containing intact acrosome, cell membrane and condensed nucleus. (**B** and **C**) Elongated spermatids from BPA 12.5 µg/kg BW/day treatment group showing perturbed membrane (white arrowhead) and acrosome (black arrowhead), (**C**) defect in acrosomal membrane (white arrowhead). (**D-F**) Apoptotic spermatids (black arrowhead) having vacuolated (star) and collapsed membrane around the nucleus in 25 µg/kg BW/day group, (**E**) engulfed spermatids, and (**F**) heavily damaged spermatid with head defects (arrowheads) and degenerated cytoplasm. Scale bar for A is 1 µm, for B-F is 2 µm.

concerns about its adverse health effects[16]. Previous studies have shown that BPA exposure has an adverse effect on daily sperm production and the structure of sperm cells[8]. BPA exposure induces sperm abnormality by crossing the blood-testis barrier and interferes with the growth and development of sperm in Wistar rat[17]. The significant amount of data are available to indicate the adverse consequences of BPA on testicular functions in adult male rats and mice. However, there is a need to generate data transposable to humans. This study was initiated in a non-human primate model common marmoset (*C. jacchus*) which is genetically similar to human.

Normal haematological and biochemical parameters were observed except an increase in the levels of LDL and cholesterol, indicating that high dose of BPA might cause adverse effects on lipid metabolism. Previous studies conducted in our laboratory showed that BPA exposure to rat during perinatal and neonatal period results in reduced testosterone level in male offsprings[6,7]. A similar effect was observed in adult marmoset upon BPA exposure, with reduced levels of testosterone. Histological analysis in the present study showed sloughing of cells into the lumen as well as a decrease in germ cell number at spermatocyte, RS and ES level that was in agreement with the previous reports[18]. Similar observations with respect to germ cell sloughing were obtained in rat model in our previous study[7].

Spermatogenesis is very dynamic and orchestrated process, in which germ cells undergo mitotic and meiotic divisions to produce ESs. Germ cells are vulnerable to external pollutants such as chemicals, drugs and radiation[19]. Our transmission electron microscopic studies indicated damages in a few of the spermatogonial cells and more of the spermatocytes upon exposure to BPA. These included condensation of chromatin material, presence of more than two nuclei, disappearance of the nuclear envelope and numerous apoptotic changes. Similar effects were induced by other compounds such as malathion[20] and cadmium[21]. BPA caused degenerative changes in the form of vacuolation, membrane thickening and deformed basement membrane. The lamina propria maintains the structural integrity of the seminiferous tubules, and it is also a part of the blood–testis barrier in healthy adult males. Anomalies in the lamina propria are often associated with many testicular diseases. The thickened lamina propria is associated with disturbed spermatogenesis[22]. An altered basement membrane structure might be a characteristic feature of functional impairment of the marmoset testis[23].

Sertoli cells are the essential component of the blood-testis barrier that maintains the microenvironment around the germ cells and facilitates spermatogenesis. These are also the sources of growth factors and nutrients, which provide energy for germ cell meiosis[23,24]. In the present study, though a decrease in Sertoli cell number was not observed, degenerative changes in Sertoli cell nucleus and cytoplasm along with perturbed Sertoli-to-Sertoli and Sertoli-to-germ cell junctions were seen in one-third of the total tubules analyzed. These abnormalities in Sertoli cells might affect the nutritional intake and normal maturation of spermatogenic cells at various stages. The similar disruption of Sertoli cell ultrastructure was described in a previous study on rats treated with indenopyridine[25] and cisplatin[26].

Leydig cells synthesize androgens that promote spermatogenesis as well as maintain secondary sexual characteristics and sexual function after getting signals from luteinizing hormone. During the process of spermatogenesis, meiosis and sperm differentiation are facilitated by androgens[27]. The androgen receptors are mainly distributed in Sertoli, Leydig and peritubular myoid cells[9]. In contrast to control group, plenty of lipid droplets were observed in Leydig cells in both the 12.5 and 25 µg/kg BW/day treated groups. The number of lipid droplets is inversely proportional to the rate of androgen synthesis[28]. The electron microscopic analysis depicted the lipid droplets in Leydig cells in the BPA-treated animals that could be a plausible reason for the reduced testosterone levels observed in the 25 µg/kg BW/day BPA-exposed group. Mitochondrial swelling and numerous lipid droplets in the Leydig cells have been observed under stress conditions in rat[29]. It has been reported that androgen deficiency disturbs spermiation process by altering spermatid-Sertoli cell junctions. This further leads to premature detachment of RSs from Sertoli cells and seminal epithelium[30]. These degenerative changes in Leydig cells may interfere with normal function and inhibit synthesis of androgens, which may further affect the spermatogenesis process.

Studies on mice and rats exposed to 20 and 200 µg/kg BW/day of BPA for six days showed transient changes in the ultrastructure of testicular cells[8]. However, similar ultrastructural effects were observed after chronic exposure (70 days) to common marmoset at 12.5 and 25 µg/kg BW/day doses of BPA. Further studies are needed to determine if the effects of BPA are reversible[8]. Likewise, swollen mitochondria and abnormal cytoplasmic contents, glycogen deposits, lipid and unusual membranous profiles were clearly evident as reported by other EDs such as dichlorodiphenyltrichloroethane, vinclozolin[31] and perfluoro-octane sulphonate[32]. A transcriptome analysis of BPA showed the differentially expressed genes being involved in important processes such as lipid metabolism, endocrine disruption and apoptosis[33].

In conclusion, the adverse effects of the chronic treatment of BPA to the testis of common marmosets were demonstrated. This study provided information about BPA-induced reproductive toxicity in the adult male model. The observed ultrastructural changes in testicular morphology might be indicative of a perturbed sperm production and functioning. Considering the genetic and spermatogenic similarities of *C. jacchus* and humans, this study would be helpful in correlating the adverse effects in humans.

Acknowledgment

Authors acknowledge the assistance provided by Sarvshri Sharad Bhagat, Jayant Tare, Pravin Salunkhe, Subhash Kadam and Mahadeo Pawar. The authors thank the Indian Council of Medical Research (Research Article/269/06-2015) and Scientific Engineering and Research Board for funding the study.

***Conflicts of Interest*:** None.

References

1. Diamanti-Kandarakis E, Bourguignon JP, Giudice LC, Hauser R, Prins GS, Soto AM, *et al.* Endocrine-disrupting chemicals: An Endocrine Society scientific statement. *Endocr Rev* 2009; *30* : 293-342.
2. De Coster S, van Larebeke N. Endocrine-disrupting chemicals: Associated disorders and mechanisms of action. *J Environ Public Health* 2012; *2012* : 713696.
3. Vandenberg LN, Colborn T, Hayes TB, Heindel JJ, Jacobs DR Jr., Lee DH, *et al.* Hormones and endocrine-disrupting chemicals: Low-dose effects and nonmonotonic dose responses. *Endocr Rev* 2012; *33* : 378-455.
4. Chitra KC, Latchoumycandane C, Mathur PP. Induction of oxidative stress by bisphenol A in the epididymal sperm of rats. *Toxicology* 2003; *185* : 119-27.
5. Sakaue M, Ohsako S, Ishimura R, Kurosawa S, Kurohmaru M, Hayashi Y, *et al*. Bisphenol A affects spermatogenesis in the adult rat even at a low dose. *J Occup Health* 2001; *43* : 185-90.
6. Salian S, Doshi T, Vanage G. Impairment in protein expression profile of testicular steroid receptor coregulators in male rat offspring perinatally exposed to bisphenol A. *Life Sci* 2009; *85* : 11-8.
7. Salian S, Doshi T, Vanage G. Perinatal exposure of rats to bisphenol A affects the fertility of male offspring. *Life Sci* 2009; *85* : 742-52.
8. Toyama Y, Suzuki-Toyota F, Maekawa M, Ito C, Toshimori K. Adverse effects of bisphenol A to spermiogenesis in mice and rats. *Arch Histol Cytol* 2004; *67* : 373-81.
9. Liu XL, Chen XY, Wang ZC, Shen T, Zhao H. Effects of exposure to bisphenol A during pregnancy and lactation on the testicular morphology and caspase-3 protein expression of ICR pups. *Biomed Rep* 2013; *1* : 420-4.
10. Millar MR, Sharpe RM, Weinbauer GF, Fraser HM, Saunders PT. Marmoset spermatogenesis: Organizational similarities to the human. *Int J Androl* 2000; *23* : 266-77.
11. Leranth C, Hajszan T, Szigeti-Buck K, Bober J, MacLusky NJ. Bisphenol A prevents the synaptogenic response to estradiol in hippocampus and prefrontal cortex of ovariectomized nonhuman primates. *Proc Natl Acad Sci U S A* 2008; *105* : 14187-91.
12. Holt WV, Moore HD. Ultrastructural aspects of spermatogenesis in the common marmoset (*Callithrix jacchus*). *J Anat* 1984; *138* (Pt 1) : 175-88.
13. National Toxicology Program (USA). *NTP-CERHR Monograph on the Potential Human Reproductive and Developmental Effects of Bisphenol A*. Available from: *https://*

ntp.niehs.nih.gov/ntp/ohat/bisphenol/bisphenol.pdf, accessed on July 20, 2017.

14. Weinbauer GF, Aslam H, Krishnamurthy H, Brinkworth MH, Einspanier A, Hodges JK. Quantitative analysis of spermatogenesis and apoptosis in the common marmoset (*Callithrix jacchus*) reveals high rates of spermatogonial turnover and high spermatogenic efficiency. *Biol Reprod* 2001; *64* : 120-6.
15. Vandenberg LN, Chahoud I, Padmanabhan V, Paumgartten FJ, Schoenfelder G. Biomonitoring studies should be used by regulatory agencies to assess human exposure levels and safety of bisphenol A. *Environ Health Perspect* 2010; *118* : 1051-4.
16. Li DK, Zhou Z, Miao M, He Y, Wang J, Ferber J, *et al.* Urine bisphenol-A (BPA) level in relation to semen quality. *Fertil Steril* 2011; *95* : 625-30.e4.
17. Wisniewski P, Romano RM, Kizys MM, Oliveira KC, Kasamatsu T, Giannocco G, *et al.* Adult exposure to bisphenol A (BPA) in Wistar rats reduces sperm quality with disruption of the hypothalamic-pituitary-testicular axis. *Toxicology* 2015; *329* : 1-9.
18. Prakash N, Vijay KM, Sunilchandra U, Pavithra B, Pawar A. Evaluation of testicular toxicity following short-term exposure to cypermethrin in albino mice. *Toxicol Int* 2010; *17* : 18-21.
19. Tripathi R, Mishra DP, Shaha C. Male germ cell development: Turning on the apoptotic pathways. *J Reprod Immunol* 2009; *83* : 31-5.
20. Penna-Videau S, Bustos-Obregón E, Cermeño-Vivas JR, Chirino D. Malathion affects spermatogenic proliferation in mouse. *Int J Morphol* 2012; *30* : 1399-407.
21. Wang L, Xu T, Lei WW, Liu DM, Li YJ, Xuan RJ, *et al.* Cadmium-induced oxidative stress and apoptotic changes in the testis of freshwater crab, *Sinopotamon henanense*. *PLoS One* 2011; *6* : e27853.
22. Volkmann J, Müller D, Feuerstacke C, Kliesch S, Bergmann M, Mühlfeld C, *et al.* Disturbed spermatogenesis associated with thickened lamina propria of seminiferous tubules is not caused by dedifferentiation of myofibroblasts. *Hum Reprod* 2011; *26* : 1450-61.
23. Mesbah SF, Shokri S, Karbalay-Doust S, Mirkhani H. Effects of nandrolone decanoate on ultrastructure of testis in male adult rats. *Iran J Med Sci* 2008; *33* : 1493-501.
24. Sharpe RM, McKinnell C, Kivlin C, Fisher JS. Proliferation and functional maturation of Sertoli cells, and their relevance to disorders of testis function in adulthood. *Reproduction* 2003; *125* : 769-84.
25. Hild SA, Reel JR, Dykstra MJ, Mann PC, Marshall GR. Acute adverse effects of the indenopyridine CDB-4022 on the ultrastructure of sertoli cells, spermatocytes, and spermatids in rat testes: Comparison to the known sertoli cell toxicant Di-n-pentylphthalate (DPP). *J Androl* 2007; *28* : 621-9.
26. Mohammadnejad D, Abedelahi A, Soleimani-Rad J, Mohammadi-Roshandeh A, Rashtbar M, Azami A. Degenerative effect of Cisplatin on testicular germinal epithelium. *Adv Pharm Bull* 2012; *2* : 173-7.
27. Lipsett MB, Wilson H, Kirschner MA, Korenman SG, Fishman LM, Sarfaty GA, *et al.* Studies on Leydig cell physiology and pathology: Secretion and metabolism of testosterone. *Recent Prog Horm Res* 1966; *22* : 245-81.
28. Azhar S, Reaven E. Regulation of Leydig cell cholesterol metabolism. In: Payne AH, Hardy MP, editors. *The Leydig cell in health and disease*. Totowa: Humana Press; 2007. p. 135-48.
29. Wang FF, Wang Q, Chen Y, Lin Q, Gao HB, Zhang P. Chronic stress induces ageing-associated degeneration in rat Leydig cells. *Asian J Androl* 2012; *14* : 643-8.
30. Beardsley A, O'Donnell L. Characterization of normal spermiation and spermiation failure induced by hormone suppression in adult rats. *Biol Reprod* 2003; *68* : 1299-307.
31. Veeramachaneni DN. Impact of environmental pollutants on the male: Effects on germ cell differentiation. *Anim Reprod Sci* 2008; *105* : 144-57.
32. Zhao B, Li L, Liu J, Li H, Zhang C, Han P, *et al.* Exposure to perfluorooctane sulfonate in utero reduces testosterone production in rat fetal Leydig cells. *PLoS One* 2014; *9* : e78888.
33. Ali S, Steinmetz G, Montillet G, Perrard MH, Loundou A, Durand P, *et al.* Exposure to low-dose bisphenol A impairs meiosis in the rat seminiferous tubule culture model: A physiotoxicogenomic approach. *PLoS One* 2014; *9* : e106245.

Reprint requests: Dr Vikas D. Dighe, National Centre for Preclinical Reproductive & Genetic Toxicology, ICMR-National Institute for Research in Reproductive Health, J.M. Street, Parel, Mumbai 400 012, Maharashtra, India
e-mail: dighev@nirrh.res.in